PCCP

Accepted Manuscript

ROYAL SOCIETY OF CHEMISTRY

www.rsc.org/pccp

Cite this: DOI: 10.1039/c0xx00000x

www.rsc.org/xxxxxx

ARTICLE TYPE

TAP study of toluene total oxidation over a Co_3O_4/La-CeO_2 catalyst with an application as washcoat of cordierite honeycomb monoliths

Diana M. Gómez[a], Vladimir V. Galvita[b*], José M. Gatica[a], Hilario Vidal[a], Guy B. Marin[b]

Received (in XXX, XXX) Xth XXXXXXXXX 20XX, Accepted Xth XXXXXXXXX 20XX

DOI: 10.1039/b000000x

The total oxidation of toluene was studied over a Co_3O_4/La-CeO_2 catalyst in a Temporal Analysis of Products (TAP) set-up in the temperature range 713 K to 873 K in the presence and absence of dioxygen. It has been demonstrated that the reaction proceeds via a Mars–van Krevelen mechanism. The reaction rate increased 8.4 times if both toluene and dioxygen were present in the feed. The partial reaction order with respect to O_2 diminished from 0.9 to 0.6 with an increase in temperature from 763 to 873 K. Adsorbed oxygen species with a lifetime of ~8s have been found on a catalyst fully oxidized by dioxygen. Catalysis of isotopically labeled $^{18}O_2/^{12}C_6H_5{}^{13}CH_3$ results in formation of products containing ^{18}O, which indicates that both lattice and adsorbed oxygen are involved in total oxidation of toluene. The role of adsorbed oxygen is activation of C-H bond in toluene. The reaction network of the catalytic total oxidation of toluene consists of the following sequence: adsorption of toluene on the catalyst surface; activation of toluene by dehydrogenation with adsorbed oxygen; oxidation of activated toluene mainly by the lattice oxygen and re-oxidation of reduced catalyst by dioxygen.

1. Introduction

The legislation of specific regulations for the control and elimination of volatile organic compounds (VOCs) has motivated the development of methods and materials for their treatment and removal. Among these methods of VOC abatement, catalytic combustion has been widely employed and is recognized as one the most efficient [1, 2].

For the total oxidation of VOCs, noble metal catalysts supported over high surface area materials exhibit excellent activity [3]. However, the high cost and low resistance to poisoning of noble metal catalysts has stimulated interest in the development of other transition metal oxide-containing catalysts as a substitute. Among the transition metal oxides, cobalt oxide has shown to be one of the most efficient for total oxidation of VOCs[4-6].

CeO_2 is widely employed as a catalytic promoter due to its redox behavior, oxygen defects, and catalytic activity which have been attributed to its peculiar oxygen storage capacity (OSC) associated with the fast Ce^{4+}/Ce^{3+} redox process [7-9]. Furthermore, the thermal stability and redox properties of CeO_2 can be enhanced by adding dopants such as La^{3+} [10, 11]. Because of these properties of CeO_2, supporting a cobalt oxide catalyst on ceria modifies its redox properties, enhances oxygen mobility, and improves its VOC oxidation activity[12-15]. Recently, it was reported that a catalyst with a Co_3O_4/La-CeO_2 formulation presented good activity and stability in the total oxidation of toluene [16].

It is generally accepted that the total oxidation of VOCs over Co_3O_4-containing catalysts occurs according to a Mars-van Krevelen mechanism [14, 17-23]. Liotta et al. [13] and Bahlawane [17] have reported that the total oxidation of methane over cobalt oxide-based catalysts takes place through a Mars–Van Krevelen mechanism involving lattice oxygen via a redox cycle. However, while studying propane oxidation, Liu et al. [23] demonstrated that highly strained cobalt-spinel nano-crystals with an enhanced lattice distortion exhibit a high catalytic activity. The authors correlated catalytic activity with the amount of chemisorbed electrophyllic O^- species. In other reports, Busca et al. [24] and Luo et al. [12] suggested that for a Co_3O_4 catalyst, the nucleophilic oxygen species were those involved in propane catalytic total oxidation. On the other hand, Liotta et al. [14] proposed that during propene oxidation, over Co_xCe oxides, both electrophilic oxygen and lattice oxygen species may participate in the reaction depending on the temperature. Similarly, Machida et al.[25] suggested that the structural defects of the lattice are linked with the creation of active surface species. This suggests a key role for CeO_2, since its oxygen transport properties are controlled by the presence of defects which could be increased by the addition of appropriate dopants like lanthanum and because its redox properties may improve the catalytic behavior of the catalyst by increasing the supply of active oxygen.

The total oxidation activity of a catalyst is determined not by regular lattice oxygen atoms, but by weakly bound forms of oxygen such as adsorbed oxygen species and/or oxygen atoms connected to the oxide surface with a low binding energy in contrast with the regular lattice oxygen atoms [26-28]. These appear on the surface of a catalyst as the result of equilibrium between the oxide lattice and the gas phase [29].

$$O_{2gas} \leftrightarrow O_{2ads} \leftrightarrow O_2^-{}_{ads} \leftrightarrow 2O^-{}_{ads} \leftrightarrow 2O^{2-}{}_{latt}$$

During steady state equilibrium, the surface of a catalyst is continuously covered by a variety of highly reactive oxygen species which are available for reaction. The role and nature of these adsorbed oxygen species in catalytic combustion over Co_3O_4-containing catalysts where they act as electrophilic oxygen and lattice "nucleophilic" oxygen is not fully clarified.

Transient response techniques with millisecond time resolution are powerful tools for the investigation of reaction steps and possible catalyst surface transformations during catalytic reactions. Temporal-Analysis-of-Products (TAP) has been recognized as an important transient experimental method for catalytic reaction studies. A TAP pulse response experiment consists of injecting a very small amount of gas (10^{14} molecules) into a fixed bed reactor that is kept under vacuum. The pressure rise in the micro-reactor is small and transport in the reactor, which is driven by a gas concentration gradient, is dominated by Knudsen diffusion. In this study, a TAP reactor is applied as a unique transient tool to investigate the role of active oxygen species in the catalytic total oxidation of toluene over a Co_3O_4/La-CeO_2 catalyst. This catalyst was selected with consideration to previous work suggesting potential application in this reaction even when supported by washcoating onto honeycomb cordierite monoliths [16]. Although the TAP technique has been widely used to obtain information on the oxidations of VOCs, scarce results have been reported for the total oxidation of toluene. Some authors have studied toluene oxidation over uranium oxide based catalysts [30], V_2O_5/TiO_2 catalysts [31], and CuO-CeO_2/Al_2O_3 [32] catalysts using a TAP reactor, but the technique has not previously been employed in the study of cobalt-containing catalysts.

2. Experimental

2.1 Catalyst preparation and characterization

Preparation of the washcoating Co_3O_4/La-CeO_2 catalyst consisted of three stages, as reported in [16]. In the first stage, the La(6.84 wt%)-CeO_2 support was prepared by incipient wetness impregnation of CeO_2 by $La(NO_3)_3 \cdot 6H_2O$ and calcined at 773 K for 4 hours. Second, the La-CeO_2 support was impregnated with an aqueous solution of $Co(CH_3COO)_2 \cdot 4H_2O$. The sample was then dried and calcined at 723 K for 2 hours to obtain the powdered cobalt catalyst. Finally, a 25 wt% solid content slurry was prepared by mixing the powdered catalyst with polyvinyl alcohol and colloidal alumina as additives, which was then calcined at 723 K for 2 h. The resulting powdered sample (named Co_3O_4/La-CeO_2), which was employed in this study resembled a corresponding catalyst supported on cordierite honeycomb monoliths investigated in [16] and nanostructurally characterized in [33]. The elemental composition (wt.%) of the calcined dried slurry as determined by ICP analysis was: Co (11.41); La (4.44); Ce (44.39); Al (7.4). Its BET surface area was determined by N_2 adsorption to be 87.8 m^2g^{-1}. Crystallographic analyses for the tested catalysts were performed by means of in situ X-ray diffraction (XRD) measurements in θ–2θ mode using a Bruker-AXS D8 Discover apparatus with Cu Kα radiation of wavelength 0.154 nm and a linear detector covering a range of 20° in 2θ with an angular resolution of approximately 0.1° in 2θ. While the minimal capturing time is 0.1 s, a collection time of typically 10 s was used during these experiments.

The evolution of the catalyst structure during TPR was investigated in a flowing gas stream (5 vol.% H_2/N_2) from room temperature to 973 K. The in situ experiments were carried out using a home-built reactor chamber with Kapton foil window for X-ray transmission. A 15 mg sample was evenly spread on a single crystal Si wafer. The sample was heated from room temperature to 973K at a heating rate of 20 K/min. Peak positions and widths were determined by means of a Gaussian function, fit to a XRD peak in a chosen range of 2θ around the peak of interest. Due to the low angular resolution of the linear detector, these values cannot yield accurate crystallite size and unit cell parameters, but they do allow tracing trends in a qualitative way.

X-ray diffraction studies (XRD) showed that the peaks corresponding to the face-centered cubic fluorite structure of CeO_2 have a slight shift in their position towards lower 2θ values with respect to those of pure ceria suggesting that the lanthanum is incorporated in the lattice of ceria. The XRD analysis also identified exhibited crystalline features of Co_3O_4 spinel. More details about the catalyst can be found in [16, 33]

2.2 Experimental set-up

The TAP reactor set-up employed in this work is described in Gleaves et al. [34]. TAP experiments are performed in a tubular reactor which is placed in vacuum (10^{-5} Pa) with a nanomole amount of reactant molecules (10^{-9} mol). The reactor is made of quartz and measures 33 mm in length with an inner diameter of 4.75 mm. The entrance of the reactor is connected with two high-speed pulse valves via a small volume. Molecules are pulsed into the reactor by means of two pulse valves and the products and the unreacted reactants are monitored by a UTI 100C quadruple mass spectrometer. The number of molecules admitted during pulse experiments amounts to ~10^{15} molecules/pulse with a pulse time of 140 μs.

In order to feed toluene into the reactor, a liquid feed set up was designed and constructed at the Laboratory for Chemical Technology, Ghent University. It consists of a liquid vaporizing chamber, which is heated to 423 K, into which the liquid feed is injected by use of a 500μL Hamilton Gastight ® #1750 syringe. Pressure is maintained at the point of injection by a Hamilton, high-temperature septum. The vaporizing chamber is also connected with gas bottles, which allows the making of gas mixtures. The temperature of the feeding lines is maintained at 423 K. The manifold assembly containing the pulse valves is kept at 348 K, the maximum temperature allowed. The pressure of the feed from the liquid feeding lines to the pulse valves is maintained at 1.2 bar as it was experimentally determined to be the pressure at which the pulse valves function best. The amount of liquid injected into the vaporizing chamber is such that a vapor state is maintained at the temperature and pressure in the manifold assembly.

Three types of experiments were carried out: single-pulse, multi-pulse and alternating pulse experiments [35, 36]. Single-pulse experiments were carried out to study the interaction of a gas with the catalyst at a particular state, by pulsing approximately 10^{14} molecules/pulse. The state of the catalyst remains unaltered during a single-pulse experiment as the number of molecules pulsed is 5 orders of magnitude less than the number of active sites in the catalyst. Typically, 5-10 responses of a particular Atomic Mass Unit (AMU) are collected and averaged in order to obtain a better signal to noise ratio. If components corresponding to different AMUs must be measured, each AMU is measured

one after another pulse for the required number of times and averaged. Multipulse experiments were performed in order to change the state of the catalyst by pulsing an amount of molecules on the order of 10^{16} molecules/pulse and collecting about 1000 responses. Multipulse experiments were used to obtain different states of the catalyst. Alternating pulse experiments were performed with various time lags between two different pulses. In general, by varying the lag times between the two pulses, the lifetime of the surface species originating from the first, i.e, the pump pulse can be determined.

2.3 Catalyst testing

Experiments were performed over 15 mg of Co_3O_4/La-CeO_2 catalyst. The catalyst was packed between two inert zones of quartz particles of the same size ($250<d_p<500\mu m$). Typically, reaction mixtures were prepared with Ar as one of the components, so that the inlet amount of the components could be determined from the Ar response. The experiments performed after re-oxidizing the catalyst were conducted within 15-20 seconds of stopping the re-oxidation. After re-oxidation by a dioxygen multipulse experiment, if the catalyst remained for an additional 10 min under vacuum at reaction temperatures, no extra oxygen uptake was seen from another dioxygen pulse.

A temperature range of 713 K- 873 K was covered. Blank measurements were conducted with toluene and dioxygen over quartz particles of the same size. No oxidation products or decomposition of toluene were observed. When required, re-oxidation of the catalyst was performed by conducting dioxygen multipulse experiments until the outlet oxygen response was steady.

For the quantification of the components of toluene total oxidation, the Mass Spectrometer was focused on different AMUs, the selection of which was based on an analysis of the mass spectra of the individual components: $C^{16}O_2$ at 44, $C^{16}O^{18}O$ at 46, $C^{18}O_2$ at 48, $^{13}CO_2$ at 45, O_2 at 32, C_7H_8 at 91, C_6H_5–$^{13}CH_3$ at 92, Ar at 40 AMU.

Typically, a stoichiometric molar ratio of dioxygen to toluene, i.e. 9:1, was used in the mixture C_7H_8/O_2/Ar, when experiments were conducted in the presence of dioxygen. To study the effect of partial pressure of dioxygen in the reaction mixture, feeds with different ratios of components in the reaction mixture C_7H_8/O_2/Ar were applied. The amount of C_7H_8 was kept constant and that of O_2 and Ar was varied. Molar ratios of C_7H_8/O_2=1:9, 1:6, 1:4, 1:2, 1:1 and 1:0 were used. Single-pulse experiments were performed with various feed mixtures on oxidized catalyst at temperatures varying from 713 K to 873 K. The partial reaction order of dioxygen, n, was calculated based on equation (1):

$$\ln[Y_{CO2}] = k + n\ln[O_2] + m\ln[C_7H_8] \qquad (1)$$

where $[Y_{CO2}]$ is the extensive molar production of CO_2 (mol) and $[O_2]$ and $[C_7H_8]$ are the amount of dioxygen and toluene in the reaction mixture (mol).

In order to study the interaction of dioxygen with the catalyst, oxygen isotopic exchange experiments were performed by pulsing mixtures of C_6H_5-$^{13}CH_3$/$^{18}O_2$/Ar over an $^{16}O_2$ pretreated catalyst and monitoring the formation of $^{12}C^{16}O_2$, $^{12}C^{18}O_2$, $^{12}C^{16}O^{18}O$, $^{13}C^{16}O_2$, $^{13}C^{18}O_2$ and $^{13}C^{16}O^{18}O$. C_7H_8/$^{18}O_2$/Ar was pulsed at high pulse intensities (~10^{14} molecules/pulse) as the sensitivity of the mass spectrometer is not high enough to measure H_2O at lower reactant pulse intensities. $^{18}O_2$ (97%, chemical purity 99.8 %) from Cambridge Isotopes Laboratories Inc. was used for the oxygen isotopic exchange experiments. The activation of C–H and C–C bonds in toluene was investigated by pulsing isotope of toluene, viz. C_6H_5–$^{13}CH_3$ (Isotec™, 99 atom% ^{13}C).

To investigate the lifetime of adsorbed oxygen species and their effect on the oxidation of toluene, alternating pulse experiments were performed with oxygen and toluene, at ~10^{15} molecules/pulse with varying time lags for the toluene pulse.

The theoretical number of exchangeable oxygen atoms in the catalyst was calculated according to the presence of Co_3O_4 and CeO_2 using following equations:

$$Co_3O_4 \Leftrightarrow 3Co+2O_2 \qquad (2)$$
$$2CeO_2 \Leftrightarrow Ce_2O_3 + 0.5O_2 \qquad (3)$$

The total number of exchangeable oxygen atoms in the Co_3O_4 and CeO_2 for the 15 mg of Co_3O_4/La-CeO_2 catalyst was calculated to be $3.85\cdot10^{19}$ molecules, i.e.,14 orders of magnitude higher than the number of molecules admitted in a single pulse.

3. Results

3.1. Toluene conversion to CO_2 in the presence and absence of dioxygen

Figure 1a and 1b show the outlet molar flow rate of C_7H_8 and CO_2 obtained by performing single-pulse experiments, pulsing C_7H_8/Ar (1a) and C_7H_8/O_2/Ar (1b) at 873 K over Co_3O_4/La-CeO_2 oxidized catalyst. A ratio of 1:9 for C_7H_8/O_2 was employed in the latter case. The amount of C_7H_8 in the feed mixture was kept the same in both experiments.

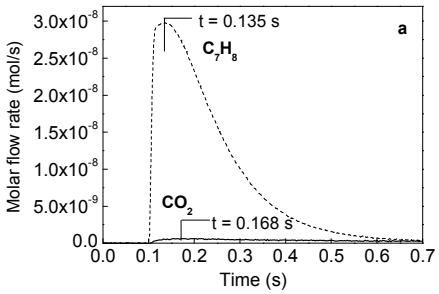

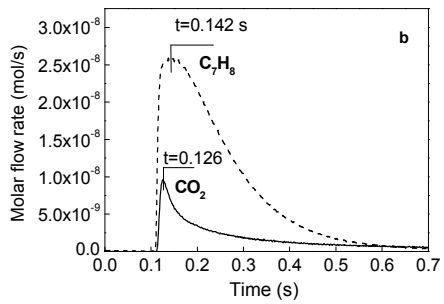

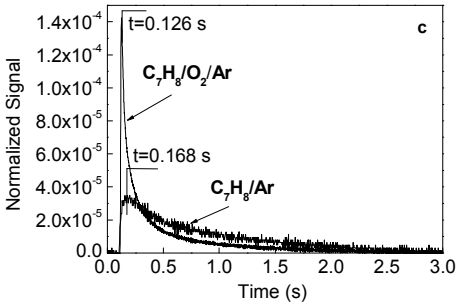

Figure 1. Molar flow rate of CO_2 (—) and C_7H_8 (- - -) versus time during single-pulse experiments with (a) C_7H_8/Ar and with (b) C_7H_8/O_2/Ar (ratio C_7H_8:O_2 1:9) over pre-oxidized Co_3O_4/La-CeO_2 at 873 K. (c) Moment-normalized TAP pulse-response for CO_2 production versus time corresponding to a single-pulse experiment with C_7H_8/Ar (- - -) and C_7H_8/O_2/Ar (—).

The behavior of toluene oxidation observed in Figure 1(a) suggests that the reaction is carried out according to a Mars-van Krevelen mechanism [37]. For each toluene molecule, four oxygen atoms are required to form water and fourteen to form CO_2. All of the required oxygen atoms were taken only from the catalyst lattice. The CO_2 response is broad and the peak maximum is at 0.168 s, which is higher than that of C_7H_8 (0.135 s). This difference cannot be explained by differences in molecular mass (44 and 92). The observed shift in the CO_2 peak and the long residence time can be attributed to the slow rate of CO_2 formation due to the diffusion of oxygen from the bulk and/or the sequence of reactions for the breakage of C-H and C-C bonds in adsorbed toluene. The long tail of the response could also result from slow desorption of CO_2 from the sample. Since CO_2 is known to interact with Al_2O_3 and CeO_2 [38, 39], experiments pulsing CO_2 over the catalyst were also performed (results not shown). In that case, the signal of the CO_2 pulse was narrower than the one corresponding to the CO_2 formed as a product of toluene total oxidation. It was also broader than that of Ar, which reflects interaction of carbon dioxide with the catalyst.

Addition of dioxygen to the reaction mixture significantly increased the formation of carbon dioxide Figure 1(b). The amount of CO_2 was 8.4 times more than the CO_2 produced from lattice oxygen only. The normalized area of carbon dioxide responses corresponding to the single-pulse experiment shows that the tails of the CO_2 response were broader for the toluene pulses without dioxygen, Figure 1(c). The CO_2 response corresponding to the experiment with toluene alone does not become flat at 3s. The surface alone cannot supply all the oxygen atoms required for total toluene oxidation. The reaction requires more oxygen atoms which must diffuse in bulk from lattice planes beneath the surface. In the experiment with a mixture of toluene and dioxygen, the latter regenerates the catalyst or directly participates in the reaction thereby increasing the CO_2 production rate. Whereas, in the experiment with toluene alone, the vacant sites at the surface must be replenished by oxygen atoms diffusing from the bulk.

An increase in the conversion of toluene to CO_2 was observed in the presence of dioxygen, so the effect of partial pressure of dioxygen in the feed mixture was investigated. The toluene oxidation was carried out with different ratios of O_2/C_7H_8 (9:1, 6:1, 4:1, 2:1, 1:1 and 0:1) at three reaction temperatures (763, 813 and 873 K) over the pre-oxidized catalyst. The partial reaction order of dioxygen in the reaction mixture is shown in Figure 2a. Increase of the temperature leads to a decrease in the order of dioxygen, with the highest value of 0.99 obtained at 763 K and the lowest value of 0.68 at 873 K. This result confirms that the influence of partial pressure of dioxygen in the reaction mixture during oxidation of toluene is more important at lower temperatures as also reported by Menon et al. [32] in the case of total oxidation of toluene over CuO based catalysts. This behavior is in agreement with a Mars–van Krevelen mechanism. At low reaction temperatures, oxygen diffusion from the catalyst bulk to the surface is a slow process and competition is observed between bulk oxygen and gas phase dioxygen in the regeneration of the vacant sites. At high temperatures, mobility of oxygen in the oxides increases and the role of dioxygen is less pronounced under TAP experimental conditions. The effect of toluene partial pressure was investigated at 763 K, 813 K, and 873 K over an oxidized catalyst and the result is plotted in Figure 2b. The partial reaction order of toluene was roughly constant, around 0.45, in the interval of temperatures studied.

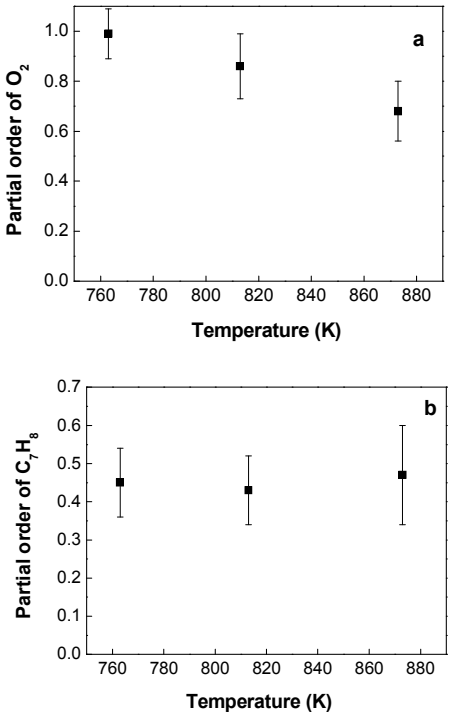

Figure 2. Partial reaction order of dioxygen (a) and toluene (b) versus temperature for single-pulse experiments performed with various feed mixtures over pre-oxidized Co_3O_4/La-CeO_2. The indicated points correspond to the average for six feed mixtures and the bars represent the standard error.

3.3. Role of adsorbed oxygen

To obtain information about the participation of adsorbed oxygen in the reaction, the $^{16}O_2$ pretreated catalyst was pulsed with a mixture of $^{12}C_6H_5$-$^{13}CH_3$ /$^{18}O_2$/Ar at 873K. This isotope of toluene was used to elucidate the sequence in which the various

C-C bonds in toluene are broken during the oxidation by gas and lattice oxygen. The first pulse response of $^{12}C^{16}O_2$, $^{12}C^{18}O_2$, $^{12}C^{16}O^{18}O$ which correspond to carbon dioxide formation from phenyl and of $^{13}C^{16}O_2$, $^{13}C^{18}O_2$, $^{13}C^{16}O^{18}O$ from methyl group are shown in Figures 3(a) and 3(b), respectively. Note that in the reaction only the response from the first pulse was used, thereby excluding memory effects of carbonaceous species on the catalytic surface originating from the series of high-intensity pulses. The preferential formation of ^{16}O containing products supports the Mars-van Krevelen mechanism as total oxidation of toluene takes place involving oxygen that comes from the support (Eq.4). However, the fractions of $^{13}CO_2$ and $^{12}CO_2$ containing either one or two ^{18}O confirm that oxygen from the gas phase is also participating in the reaction (Eq.5 and 6).

$$C_6H_5CH_3 + 18^{16}O_L \rightarrow 7C^{16}O_2 + 4H_2{}^{16}O + 18V_o \quad (4)$$

$$^{18}O_2 + 2s \rightarrow 2^{18}Os \quad (5)$$

$$C_6H_5CH_3 + 18^{18}O_s \rightarrow 7C^{18}O_2 + 4H_2{}^{18}O \quad (6)$$

Where $^{16}O_L$ -lattice oxygen, $^{18}O_2$ – dioxygen in gas phase; $^{18}O_s$-adsorbed oxygen; V_o – oxygen vacancy, s- surface site.

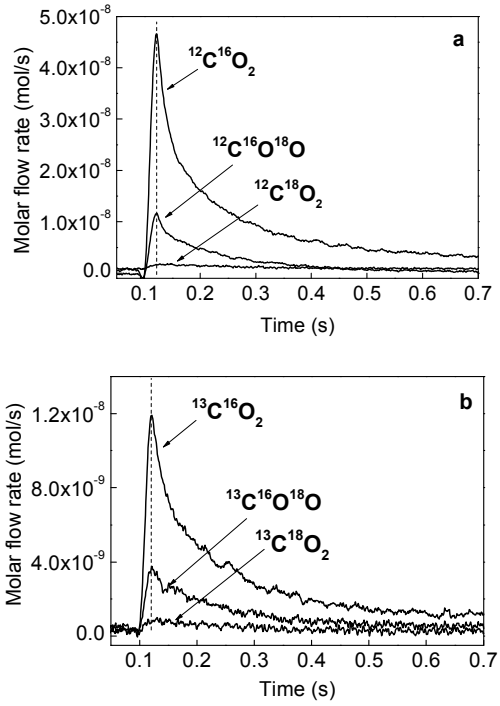

Figure 3. Molar flow rate of (a) $^{12}C^{16}O_2$, $^{12}C^{18}O_2$, $^{12}C^{16}O^{18}O$ and (b) $^{13}C^{16}O_2$, $^{13}C^{18}O_2$, $^{13}C^{16}O^{18}O$ versus time from the first pulse of a multipulse experiment with C_6H_5-$^{13}CH_3$/$^{18}O_2$/Ar over 15 mg of $^{16}O_2$ pretreated catalyst at 873 K. For the sake of clarity, signals related to ^{12}C and ^{13}C (obtained in the same experiment) have been shown separately.

Analysis of the different combinations of response products ($^{12}C^{16}O_2$ and $^{13}C^{18}O_2$; $^{13}C^{16}O_2$ and $^{13}C^{18}O_2$; $^{12}C^{16}O^{18}O$ and $^{13}C^{16}O^{18}O$) shows peaks at the same time, which means that these products are formed nearly at the same time. This could be due to the simultaneous abstraction of both methyl and phenyl carbons or because the long lifetime of carbon dioxide originated from either carbons on the catalyst surface. The fractions of $^{13}CO_2$ and $^{12}CO_2$ containing either one or two ^{18}O were 37% and 29% respectively, suggesting that the oxidation of ^{13}C-labeled methyl group is slightly favored in comparison with that of ^{12}C-labeled phenyl group.

Figure 4 shows the amount of carbon dioxide formation vs. time during a multi-pulse (1000 pulses) experiment with C_7H_8/$^{18}O_2$/Ar on a $^{16}O_2$ pretreated catalyst at 873 K. The amount of $C^{16}O_2$ decreases significantly due to the fast consumption of surface ^{16}O species. Formation of ^{18}O containing products increases with time, as surface oxygen gradually gets replaced by ^{18}O from the gas phase. The amount of $C^{16}O^{18}O$ reaches a maximum and then slowly decreases. This long tail is due to the slow diffusion of ^{16}O from the bulk to the surface Finally, $C^{18}O_2$ becomes the main reaction product. The total amount of ^{16}O in the products after 1000 pulses is 7.2% of the total amount of exchangeable ^{16}O in the catalyst.

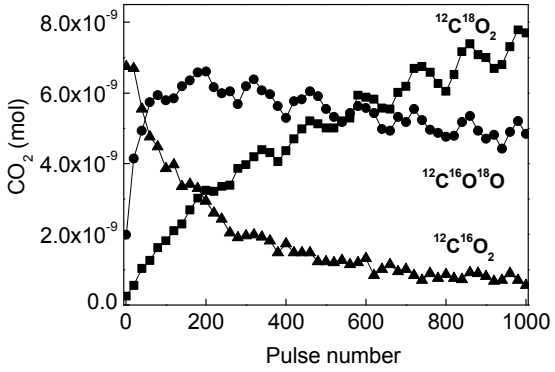

Figure 4. Amount of $^{12}C^{18}O_2$, $^{12}C^{18}O^{16}O$ and $^{12}C^{16}O_2$ formed versus time during a multipulse experiment with C_6H_5-$^{13}CH_3$/$^{18}O_2$/Ar over 15 mg of $^{16}O_2$ pretreated catalyst at 873 K.

In order to understand the contribution of secondary isotopic exchange in the product distribution (Eq. 7 and 8), $C^{18}O_2$/Ar was pulsed to the catalyst, and the amount of ^{16}O in the carbon dioxide was monitored at the outlet.

$$C^{18}O_2 + {}^{16}O_L \Leftrightarrow C^{18}O^{16}O + {}^{18}O_L \quad (7)$$

$$C^{18}O^{16}O + {}^{16}O_L \Leftrightarrow C^{16}O_2 + {}^{18}O_L \quad (8)$$

where $^{16}O_L$ and $^{18}O_L$ are lattice oxygen.

Figure 5 shows the amount of carbon dioxide formation versus time during a multipulse (1000 pulses) experiment with isotopically labeled $^{12}C^{18}O_2$/Ar over $^{16}O_2$ pretreated catalyst. The amount of $^{12}C^{16}O^{18}O$ at the outlet was 7 % of the total amount of CO_2 which confirmed that the exchange of lattice ^{16}O with ^{18}O from $C^{18}O_2$ was not significant.

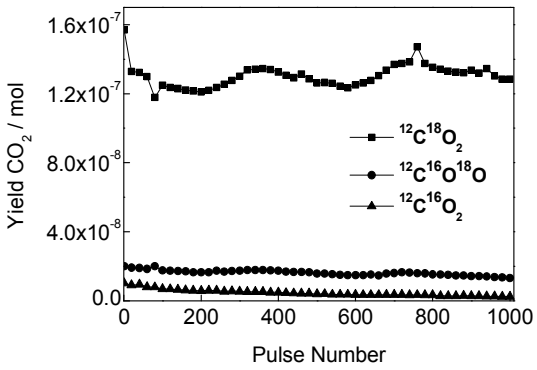

Figure 5. Amount of $^{12}C^{18}O_2$, $^{12}C^{18}O^{16}O$ and $^{12}C^{16}O_2$ formed versus time during a multipulse experiment with labeled isotopically $^{12}C^{18}O_2$/Ar over 15 mg of $^{16}O_2$ pretreated catalyst at 873 K.

3.4. Lifetime of active surface oxygen species

As described in the previous sections, two types of oxygen species are present on the Co_3O_4/La-CeO_2 catalyst: lattice oxygen are present next to adsorbed oxygen species produced from gas-phase O_2. The presence of adsorbed oxygen species and weakly bound oxygen in the lattice and their role in the oxidation of toluene was studied by performing alternating pulse experiments in which dioxygen was used as pump molecule and toluene as probe molecule. The time lag of the toluene pulse was varied after the injection of dioxygen pulse whereas the time from the injection of the toluene pulse to the next dioxygen pulse, i.e., the data acquisition time of the toluene response, was kept constant at 15 s. This was done to ensure that toluene remained over the catalyst for the same amount of time during experiments with different toluene pulse lag times. Thereby a similar catalytic state for the dioxygen pulse was maintained in all experiments.

The yield of CO_2 formed from the toluene pulse decreased with increasing time lag of the toluene pulse, as seen in Figure 6a. This can be attributed to the long lifetime of active surface oxygen species from the foregoing dioxygen pulse. The experimental data for time lag of the toluene pulse equal to 20 and 40 s was measured by pulsing $C_6H_5CH_3$/Ar after re-oxidizing the catalyst within 20 and 40 seconds of stopping the re-oxidation. The CO_2 yield in this experiment was equal to the result presented in Fig 1a. Assuming first order desorption kinetics, the lifetime of the oxygen species was calculated to be of the order of 8 s (Figure 6b), in contrast with the report of Menon et al.[32] where the lifetime of weakly bounded oxygen was only 1s during toluene total oxidation over CuO-CeO_2/Al_2O_3. A very short lifetime of the weakly bound oxygen species (≤ 10 ms) was also observed over the same CuO-CeO_2/Al_2O_3 during propane total oxidation [38]. This observed difference in the lifetime of the oxygen species can be attributed to the difference in the catalyst's active components. The O_2-TPD profiles of Co_3O_4-CeO_2, CeO_2, and CuO-CeO_2 showed oxygen desorption peaks in the temperature region below 973 K [12]. Two oxygen desorption peaks at 453 K and 857 K were observed for the Co_3O_4-CeO_2 catalyst, which could be attributed to oxygen desorption from cobalt sites since no oxygen was desorbed from pure CeO_2. In the case of CuO-CeO_2 only one peak at 907 K was observed. Quantitatively, the amount of desorbed oxygen was at least five times lower for CuO-CeO_2. This could be the result of the lower lifetime of adsorbed oxygen in the copper catalytic system.

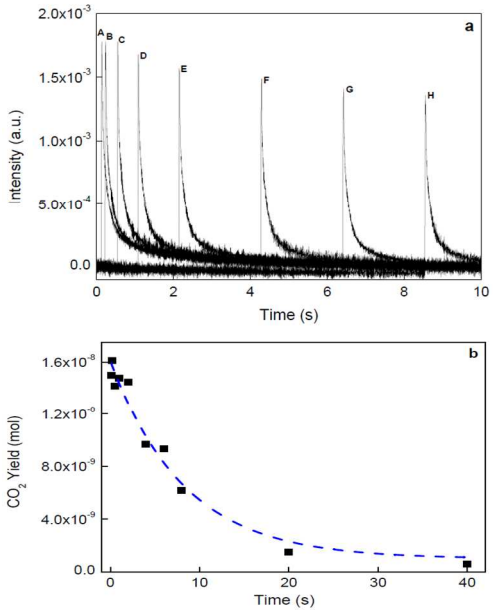

Figure 6. (a) CO_2 responses versus time during the during O_2 and C_7H_8/Ar alternating-pulse experiments with different time delays of the C_7H_8/Ar pulse over 15 mg of $^{16}O_2$ pre-treated catalyst at 873 K. Time delays of the C_7H_8/Ar pulse: 0.11 s (A), 0.2 s (B), 0.5 s (C), 1 s (D), 2 s (E), 4s (F), 6 s (G), and 8 s (H)
(b) Yield of CO_2 formed from the toluene pulse versus time during O_2 and C_7H_8/Ar alternating-pulse experiments with different time delays of the C_7H_8/Ar pulse. The dashed line is fit to a yield of CO_2 decay.

4. Discussion

The central issue addressed in this study is the role of the adsorbed and lattice oxygen species in catalytic combustion of toluene over Co_3O_4/La-CeO_2 catalysts. Pulse experiments with toluene and a mixture of toluene and dioxygen indicated different types of oxygen atoms on the catalytic surface are active in the reaction. If toluene is introduced alone, lattice oxygen from the surface and bulk is consumed to oxidize toluene to CO_2 and H_2O. These results indicate that the reaction proceeds via a classical redox Mars-van Krevelen mechanism. Adsorbed oxygen atoms are formed if dioxygen is mixed with the toluene pulse, this significantly enhancing the catalytic activity. The addition of dioxygen to the gas phase increases production of CO_2 in quantities 8.4 times higher than the CO_2 produced from lattice oxygen only. However, isotopic experiments revealed that the evolved CO_2 is principally derived from lattice oxygen. The fractions of $^{13}CO_2$ and $^{12}CO_2$ containing either one or two ^{18}O were 37% and 29% respectively. This is significantly lower than the value to be expected taking into account the increase of catalytic activity and the presence of dioxygen. Menon et al. [32]

reported that the fraction of CO_2 containing either one or two ^{18}O was 18% of the total CO_2 formed during the total oxidation of toluene over a $CuO\text{-}CeO_2/Al_2O_3$ catalyst where labeled oxygen was used. It was shown that $CuO\text{-}CeO_2/Al_2O_3$ at high temperature (>773K) and in a vacuum is thermally reduced at a high rate and the formation of ^{18}O products can be attributed to the fast re-oxidation of mildly reduced copper oxide by $^{18}O_2$ and reaction of incorporated labeled oxygen into the lattice. However, compared to the $CuO\text{-}CeO_2/Al_2O_3$ catalyst, the multipulse experiment with dioxygen over $Co_3O_4/La\text{-}CeO_2$ exposed at 873 K in a vacuum for 10 minutes did not show significant consumption of O_2. Taking into account that thermal decomposition of Co_3O_4 to CoO with O_2 release is observed above 1153 K [13], the thermal reduction of the catalyst under experimental conditions can be ignored. However, the low amount of ^{18}O in the product cannot be explained by a secondary isotopic exchange reaction. As demonstrated in Figure 5, secondary isotopic exchange did not contribute to the low amount of ^{18}O in the carbon dioxide.

High oxygen mobility and generation of active oxygen species activated by oxygen vacancies in the oxides are widely recognized as the main factors influencing the catalytic activity of Co_3O_4 and Co_3O_4–CeO_2 binary oxides for catalytic oxidation of VOCs [21, 40]. For propene oxidation, Haber and Turek [29] found that the highest rate of isotopic oxygen exchange is observed on the surface of Co_3O_4, which indicates that the surface of this oxide shows the highest coverage with electrophilic oxygen species. Liu and co-workers [23] proposed that the concentration of superficial electrophilic oxygen species is important for achieving high catalytic activity. It has been reported that oxygen vacancies on the surface of Co_3O_4 spinel lattice play an important and favorable role in accelerating the adsorption and dissociation of oxygen molecules resulting in the formation of highly active electrophilic O^- species [41, 42]. Yan et al. [43] reported that the high relative concentration surface-adsorbed oxygen on the nanoflower surface of Co_3O_4 is highly active in the oxidation of toluene due to its higher mobility than lattice oxygen. However the activation of hydrocarbons on the surface of metal oxide catalysts is the first and can be a rate-determining step of their partial or total oxidation. In every hydrocarbon molecule, the C-H bonds broken first are those characterized by lower dissociation energy [44], which are usually stronger than those of the intermediate products. In the case of toluene oxidation, that bond corresponds to the methyl group. Menon et al. [32] reported that isotopic labeling experiments with C_6H_5–$^{13}CH_3$ indicate the abstraction of the methyl carbon followed by the destruction of the aromatic ring. Furthermore, de Rivas and co-workers [45] stated that for toluene combustion, the activation of C-H bond was facilitated by surface oxygen species.

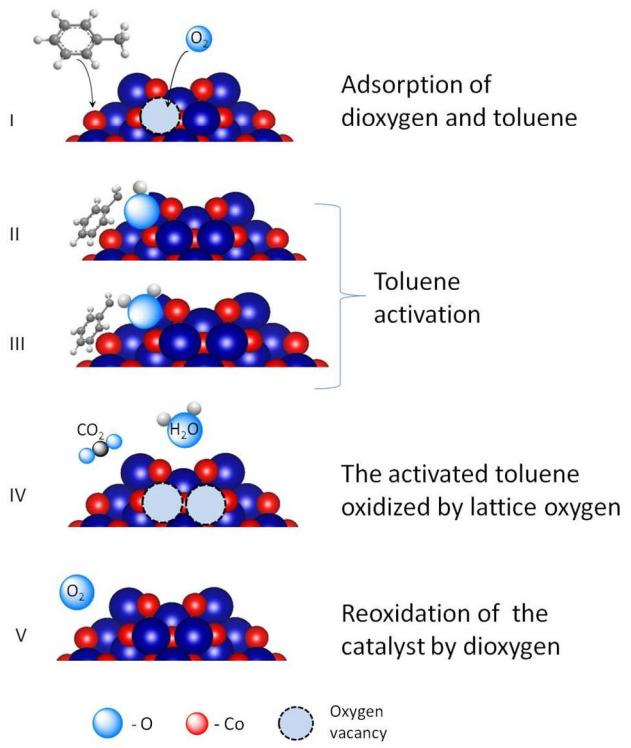

Figure 7. Schematic representation of the role of adsorbed oxygen and lattice oxygen in the total oxidation of toluene over $Co_3O_4/La\text{-}CeO_2$.

Regarding $Co_3O_4\text{-}CeO_2$ systems, Liotta et al. have reported that the oxidation of propene is governed by electrophilic oxygen species, which are transiently produced by oxygen adsorption on the surface reduced defects of ceria [14]. They have also shown that the oxidation of toluene is determined by the participation of surface oxygen species and high mobile bulk oxygen where the active species seems to be the Co_3O_4 phase whose properties were strongly modified by interaction with ceria [15]. Moreover, Luo et al. have reported that propane oxidation takes place on neighboring surface lattice oxygen sites in Co_3O_4 crystallites while CeO_2 is only physically involved in propane oxidation [12]. Although the active phase involved in the oxidation reaction is Co_3O_4, the interaction between Co_3O_4 and CeO_2 must enhance the catalytic activity since both components possess strong redox ability since the catalysis nature of VOC oxidation is redox process.

The activity of the $Co_3O_4/La\text{-}CeO_2$ catalyst in toluene oxidation can be attributed to the formation of adsorbed oxygen species when dioxygen is present in the gas phase. The adsorbed oxygen species is the main path for toluene activation on Co_3O_4 in contrast to CuO where it is lattice oxygen [32]. Based on the above analysis of the literature and experimental data, a schematic representation of the role of the different types of oxygen in toluene total oxidation over $Co_3O_4/La\text{-}CeO_2$ is given in Figure 7.

(I) Adsorption of O_2 at the vacancy and formation of highly active adsorbed oxygen species;

(II) Activation of the toluene by dehydrogenation of its weak CH_3 group by adsorbed oxygen and formation of the hydroxyl group;
(III) Hydrogen abstraction by the hydroxyl group and water formation;
(IV) Oxidation of activated toluene mainly by lattice oxygen;
(V) Re-oxidation of reduced catalyst by dioxygen.

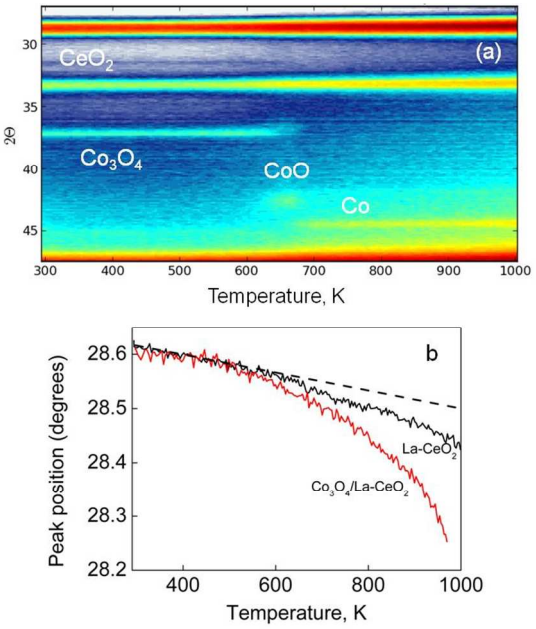

Figure 8. (a) 2D XRD pattern recorded during H_2-TPR for Co_3O_4-La-CeO_2; (b) CeO_2(111) position from XRD during H_2-TPR for the Co_3O_4-La-CeO_2 and La-CeO_2 catalyst; All TPR measuring conditions: 20 K/min; 10%H_2/N_2. Dashed line represents the peak shift due to thermal lattice expansion.

In order to understand the effect of La-CeO_2 on toluene total oxidation over the Co_3O_4 catalyst, additional in situ XRD experiments during H_2-TPR of La-CeO_2 and Co_3O_4-La-CeO_2 catalysts have been conducted. The reduction of Co_3O_4 to metallic Co can be expressed by the following consecutive reaction scheme: $Co_3O_4 \rightarrow CoO \rightarrow Co$. Upon interaction of hydrogen with ceria, two stable cerium oxidation states, Ce^{3+} and Ce^{4+}, have been observed. For the mixed materials, time-resolved XRD during H_2-TPR was performed to interpret their reducibility. The 2D diffraction pattern for the catalyst reduction is shown in Figure 8a. For Co_3O_4-La-CeO_2, Co_3O_4 and CeO_2 diffractions are visible at room temperature. During reduction, the Co_3O_4 diffractions evolve from 573 K on into CoO peaks, and finally into Co above 683K °C. Characteristic peaks associated with crystalline CeO_2 appear in all patterns of Co_3O_4-La-CeO_2 and remain visible throughout H_2-TPR. Peaks of the reduced phase Ce_2O_3 are never observed, but a possible partial reduction is checked from the position of the CeO_2(111) diffraction Figure, 8b. In Co_3O_4-La-CeO_2, its peak position as a function of temperature starts with a monotonous slope, reflecting the peak shift due to thermal lattice expansion. At temperatures above 300 °C, an additional downward deviation starts to develop, due to the onset of reduction. This indicates that, from this temperature on, part of Ce is already being reduced from 4+ to 3+. For the La-CeO_2 catalyst, the deviation from the straight CeO_2 curve starts at 673 K. This early CeO_2 reducing in case of Co_3O_4-La-CeO_2 can be due to a CeO_2 fraction connected to Co_3O_4 which re-oxidizes partially reduced cobalt species[40] (Eq. 9).

$$Co^{2+} + Ce^{4+} \rightarrow Co^{3+} + Ce^{3+} \qquad (9)$$

The interaction between Co^{3+}/Co^{2+} and Ce^{4+}/Ce^{3+} couples has been proposed to take place at boundaries of CeO_2, which leading to valence changes of cobalt species, similar to the interaction between CuO and CeO_2[46].

Conclusions

A transient kinetic study of the total oxidation of toluene has been conducted on a Co_3O_4/La-CeO_2 catalyst, washcoating of cordierite honeycomb monoliths. The reaction of total toluene oxidation proceeds through a Mars–Van Krevelen mechanism. Adsorbed oxygen species have been found when dioxygen is present in gas phase. The reaction rate significantly (8.4 times) increases if toluene and dioxygen are present in the feed compared to toluene alone. The lifetime of the adsorbed oxygen species on the catalyst surface is close to 8s. Isotopic labeling experiments using $^{18}O_2/^{12}C_6H_5{}^{13}CH_3$ indicate that the role of adsorbed oxygen is activation of a C-H bond in toluene. The adsorbed oxygen species proved main path for toluene activation on Co_3O_4 in contrast to CuO where it is lattice oxygen. Oxidation of activated toluene is carried out mainly by lattice oxygen. We propose that the reaction network of the catalytic total oxidation of toluene consists of the following sequence: adsorption of toluene on the catalyst surface; activation of toluene by dehydrogenation with adsorbed oxygen; oxidation of activated toluene mainly by the lattice oxygen, re-oxidation of reduced catalyst by dioxygen.

Acknowledgments

This work was supported by the 'Long Term Structural Methusalem Funding by the Flemish Government. The authors also thank the financial support by the Ministry of Science and Innovation of Spain/FEDER Program of the EU (Project MAT2008-00889/NAN), and the Junta de Andalucía (Group FQM-110). Prof. M. Montes and Dr. O. Sanz are acknowledged for their kind help in the sample preparation at the Applied Chemistry labs of UPV/EHU.

[a]Departamento Ciencia de los Materiales e Ingeniería Metalúrgica y Química Inorgánica, Universidad de Cádiz, 11510 Puerto Real, Spain;
[b]Ghent University, Laboratory for Chemical Technology, Technologiepark 914, B-9052 Gent, Belgium;
*Corresponding autor e-mail: vladimir.galvita@ugent.be

References

1 J. J. Spivey, *Ind. Eng. Chem. Res.,* 1987, **26**, 2165-2180.

2 J. N. Armor, *Appl. Catal. B-Environ.,* 1992, **1**, 221-256.
3 L. F. Liotta, *Appl. Catal. B-Environ.,* 2010, **100**, 403-412.
4 G. Busca, M. Daturi, E. Finocchio, V. Lorenzelli, G. Ramis and R. Willey, *Catal. Today,* 1997, **33**, 239-249.
5 F. Wyrwalski, J. -. Lamonier, S. Siffert and A. Aboukaïs, *Appl. Catal. B-Environ.,* 2007, **70**, 393-399.
6 B. Solsona, I. Vázquez, T. Garcia, T. E. Davies and S. H. Taylor, *Catal. Lett.,* 2007, **116**, 116-121.
7 A. Trovarelli, C. de Leitenburg, M. Boaro and G. Dolcetti, *Catal. Today,* 1999, **50**, 353-367.
8 M. Mogensen, N. M. Sammes and G. A. Tompsett, *Solid State Ionics,* 2000, **129**, 63-94.
9 m. Yashima, in *in Catalysis by Ceria and Related Materials,* ed. ed. A. Trovarelli, Imperial College Press, London, 2013, pp.1-45.
10 G. Colon, J. A. Navio, R. Monaci and I. Ferino, *Phys. Chem. Chem. Phys.,* 2000, **2**, 4453-4459.
11 M. G. Cutrufello, I. Ferino, R. Monaci, E. Rombi, G. Colón and J. A. Navío, *Phys. Chem. Chem. Phys.,* 2001, **3**, 2928-2934.
12 J. Luo, M. Meng, Y. Zha and L. Guo, *J. Phys. Chem.,* 2008, **112**, 8694-8701.
13 L. F. Liotta, G. Di Carlo, G. Pantaleo, A. M. Venezia and G. Deganello, *Appl. Catal. B-Environ.,* 2006, **66**, 217-227.
14 L. F. Liotta, M. Ousmane, G. Di Carlo, G. Pantaleo, G. Deganello, G. Marci, L. Retailleau and A. Giroir-Fendler, *Appl. Catal. A-Gen.,* 2008, **347**, 81-88.
15 L. F. Liotta, M. Ousmane, G. Di Carlo, G. Pantaleo, G. Deganello, A. Boreave and A. Giroir-Fendler, *Catal. Lett.,* 2009, **127**, 270-276.
16 D. M. Gómez, J. M. Gatica, J. C. Hernández-Garrido, G. A. Cifredo, M. Montes, O. Sanz, J. M. Rebled and H. Vidal, *Appl. Catal. B-Environ.,* 2014, **144**, 425-434.
17 N. Bahlawane, *Appl. Catal. B-Environ.,* 2006, **67**, 168-176.
18 B. Solsona, T. García, G. J. Hutchings, S. H. Taylor and M. Makkee, *Appl. Catal. A-Gen.,* 2009, **365**, 222-230.
19 V. P. Santos, M. F. R. Pereira, J. J. M. Órfão and J. L. Figueiredo, *Appl. Catal. B-Environ.,* 2010, **99**, 353-363.
20 H. C. Genuino, S. Dharmarathna, E. C. Njagi, M. C. Mei and S. L. Suib, *J Phys Chem C,* 2012, **116**, 12066-12078.
21 S. Todorova, A. Naydenov, H. Kolev, J. P. Holgado, G. Ivanov, G. Kadinov and A. Caballero, *Appl. Catal. A-Gen.,* 2012, **413–414**, 43-51.
22 E. Finocchio, R. J. Willey, G. Busca and V. Lorenzelli, *J. Chem. Soc. , Faraday Trans.,* 1997, **93**, 175-180.
23 Q. Liu, L. Wang, M. Chen, Y. Cao, H. He and K. Fan, *J. Catal.,* 2009, **263**, 104-113.
24 E. Finocchio, G. Busca, V. Lorenzelli and V. S. Escribano, *J. Chem. Soc. , Faraday Trans.,* 1996, **92**, 1587-1593.
25 M. Machida, Y. Murata, K. Kishikawa, D. Zhang and K. Ikeue, *Chem. Mater.,* 2008, **20**, 4489-4494.
26 S. Minicò, S. Scirè, C. Crisafulli, R. Maggiore and S. Galvagno, *Appl. Catal. B-Environ.,* 2000, **28**, 245-251.
27 S. Scirè, S. Minicò, C. Crisafulli and S. Galvagno, *Catal. Commun.,* 2001, **2**, 229-232.
28 H. Rajesh and U. S. Ozkan, *Ind. Eng. Chem. Res.,* 1993, **32**, 1622-1630.
29 J. Haber and W. Turek, *J. Catal.,* 2000, **190**, 320-326.
30 S. H. Taylor, C. S. Heneghan, G. J. Hutchings and I. D. Hudson, *Catal. Today,* 2000, **59**, 249-259.
31 C. Freitag, S. Besselmann, E. Löffler, W. Grünert, F. Rosowski and M. Muhler, *Catal Today,* 2004, **91–92**, 143-147.
32 U. Menon, V. V. Galvita and G. B. Marin, *J. Catal.,* 2011, 283, 1-9.
33 J. C. Hernández-Garrido, D. M. Gómez, D. Gaona, H. Vidal, J. M. Gatica, O. Sanz, J. M. Rebled, F. Peiró and J. J. Calvino, *J. Phys. Chem. C,* 2013, **117**, 13028-13036.
34 J. T. Gleaves, G. Yablonsky, X. Zheng, R. Fushimi and P. L. Mills, *J. Mol. Catal. A-Chem.,* 2010, **315**, 108-134.
35 G. S. Yablonsky, M. Olea and G. B. Marin, *J. Catal.,* 2003, **216**, 120-134.
36 J. Pérez-Ramírez and E. V. Kondratenko, *Catal. Today,* 2007, **121**, 160-169.
37 P. Mars and D. W. van Krevelen, *Chem. Eng. Sci.,* 1954, **3**, Supplement 1, 41-59.
38 V. Balcaen, R. Roelant, H. Poelman, D. Poelman and G. B. Marin, *Catal Today,* 2010, **157**, 49-54.
39 A. Bueno-López, K. Krishna and M. Makkee, *Appl. Catal. A-Gen.,* 2008, **342**, 144-149.
40 L. F. Liotta, H. Wu, G. Pantaleo and A. M. Venezia, *Catal. Sci. Technol,* 2013, **3**, 3085-3102.
41 H. Wu, L. Wang, Z. Shen and J. Zhao, *J. Mol. Catal. A-Chem.,* 2011, **351**, 188-195.
42 M. M. Schubert, S. Hackenberg, A. C. van Veen, M. Muhler, V. Plzak and R. J. Behm, *J. Catal.,* 2001, **197**, 113-122 .
43 Q. Yan, X. Li, Q. Zhao and G. Chen, *J. Hazard. Mater.,* 2012, **209–210**, 385-391.
44 E. Finocchio, G. Busca, V. Lorenzelli and R. J. Willey, *J. Catal.,* 1995, **151**, 204-215.
45 B. de Rivas, J. I. Gutiérrez-Ortiz, R. López-Fonseca and J. R. González-Velasco, *Appl. Catal. A-Gen.,* 2006, **314**, 54-63.
46 U. Menon, H. Poelman, V. Bliznuk, V. V. Galvita, D. Poelman and G. B. Marin, *J. Catal.,* 2012, **295**, 91-103.